Tubular epithelial NF-{kappa}B activity regulates ischemic AKI

Marko, L., Vigolo, E., Hinze, C., Park, J.K., Roel, G., Balogh, A., Choi, M., Wuebken, A., Cording, J., Blasig, I.E., Luft, F.C., Scheidereit, C., Schmidt-Ott, K.M., Schmidt-Ullrich, R., Mueller, D.N.

This is the final version of the accepted manuscript. The original article has been published online before print on 28 January 2016 and in final edited form in:

Journal of the American Society of Nephrology
2016 SEP ; 27(9): 2658-2669
doi: 10.1681/ASN.2015070748

Publisher: American Society of Nephrology

Tubular Epithelial NF-κB Activity Regulates Acute Ischemic Kidney Injury

Lajos Markó[1,2*] MD, PhD, Emilia Vigolo[2*] MSc, Christian Hinze[2] MD, Joon-Keun Park[3] PhD, Giulietta Roël[2] PhD, András Balogh[1,2] MD, PhD, Mira Choi[1] MD, Anne Wübken[2] MSc, Cording Jimmi[4] PhD, Ingolf E. Blasig[4] PhD, Friedrich C. Luft MD[1,2], Claus Scheidereit[2] PhD, Kai M. Schmidt-Ott[2#] MD, PhD, Ruth Schmidt-Ullrich[2#] PhD, Dominik N. Müller[1,2#] PhD

*These authors contributed equally to this work.

[#]Shared authorship of principal investigators.

The authors have declared that no conflict of interest exists.

[1]Experimental and Clinical Research Center, a joint cooperation between the Charité Medical Faculty and the Max-Delbrück Center for Molecular Medicine, Berlin, Germany

[2]Max-Delbrück Center for Molecular Medicine, Berlin, Germany

[3]Hannover Medical School, Hannover, Germany

[4]Leibniz-Institut für Molekulare Pharmakologie, Berlin, Germany

Word count of manuscript: 2996

Word count of the abstract: 199

Corresponding Authors:

Dr. Lajos Markó, Experimental and Clinical Research Center, Lindenberger Weg 80, 13125 Berlin, Germany, Tel: +49 30-450-540-558, Fax: +49 30-450-540-944, E-mail: lajosmarko@yahoo.com

Dr. Kai M. Schmidt-Ott, Max Delbrück Center for Molecular Medicine, Robert-Rössle-Str. 10, 13125 Berlin, Email: kai.schmidt-ott@mdc-berlin.de

Dr. Ruth Schmidt-Ullrich, Max Delbrück Center for Molecular Medicine, Robert-Rössle-Str. 10, 13125 Berlin, Email: rschmidt@mdc-berlin.de

Dr. Dominik N. Müller, Experimental and Clinical Research Center, Lindenberger Weg 80, 13125 Berlin, Germany, Tel: +49 30-450-540-286, Fax: +49 30-450-540-944, E-mail: dominik.mueller@mdc-berlin.de

ABSTRACT

NF-κB is a key regulator of innate and adaptive immunity and is implicated in the pathogenesis of acute kidney injury (AKI). The cell type-specific functions of NF-κB in the kidney are unknown; however, the pathway serves distinct functions in immune and tissue-parenchymal cells. We analyzed tubular epithelial-specific NF-κB signaling in a mouse model of ischemia-reperfusion injury (IRI)-induced AKI. NF-κB reporter activity and nuclear localization of phosphorylated NF-κB subunit p65 analyses in mice revealed widespread NF-κB activation in renal tubular epithelia and in interstitial cells following IRI that peaked at 2-3 days after injury. To genetically antagonize tubular epithelial NF-κB activity, we generated mice expressing the human NF-κB super-repressor IκBαΔN in renal proximal, distal, and collecting duct epithelial cells. These mice were protected from IRI-induced AKI, as indicated by improved renal function, reduced tubular apoptosis, and attenuated neutrophil and macrophage infiltration. Tubular NF-κB-dependent gene expression profiles revealed temporally distinct functional gene clusters for apoptosis, chemotaxis, and morphogenesis. Primary proximal tubular cells isolated from IκBαΔN-expressing mice exposed to hypoxia-mimetic agent cobalt chloride were protected from apoptosis and expressed reduced levels of chemokines. Our results indicate that postischemic NF-κB activation in renal-tubular epithelia aggravates tubular injury and exacerbates a maladaptive inflammatory response.

INTRODUCTION

Acute kidney injury (AKI) is common, affects >13 million people per year worldwide, and causes about 1.7 million deaths yearly.[1, 2] Ischemia is frequently involved and an inflammatory response to sterile cell death or injury is common.[3] The transcription factor NF-κB controls a large number of cellular processes, including immune and inflammatory responses, cell proliferation and migration, apoptosis and differentiation. The mammalian NF-κB family consists of five members p65 (RelA), c-Rel, RelB, p50/p105 (NF-κB1), and p52/p100 (NF-κB2) that form various hetero- or homodimers.[4] In the absence of any stimuli, NF-κB is sequestered in the cytoplasm by NF-κB inhibitors (IκBs). Specific stimuli lead to phosphorylation of IκB proteins by the IκB kinase complex (IKK), which results in ubiquitination and degradation of IκBs and subsequent translocation of NF-κB to the nucleus.[4, 5] NF-κB binds to specific sequences in the promoter or enhancer regions of target genes, which include genes encoding proinflammatory effectors as well as of IκB proteins to restore the steady state.[6] The p65-p50 dimer (here referred to as NF-κB) is the heterodimer that is most frequently activated by a wide range of stimuli relevant to kidney injury, including cytokines and growth factors, pathogen-associated damage and metabolic stress.[7] Several approaches have previously been employed to elucidate the role of NF-κB in AKI, including an NF-κB decoy strategy in rat kidney allograft transplantation[8] and rat renal ischemia reperfusion injury[9], or systemic administration of small-interfering RNAs targeting RelB[10] or IKKβ [11] in murine AKI models. However, NF-κB was inhibited in all cell types in these models, thereby providing only limited information about cell-specific NF-κB functions in the kidney during AKI. Previous studies in intestine and skin have highlighted the importance of distinguishing the effects of NF-κB in immune cells and in tissue parenchymal cells.[12] While NF-κB signaling is frequently pro-inflammatory[13-15], intestinal epithelial-specific or keratinocyte-specific NF-κB inhibition also can promote repair, indicating a substantial complexity of the cell type-specific NF-κB functions.[16, 17]

We aimed to determine the *in vivo* time course of NF-κB activation and its function in renal tubular epithelial cells during ischemic AKI. To assess the *in vivo* time course, we generated an NF-κB reporter mouse model in which the luciferase gene is controlled by NF-κB. Furthermore, a mouse model with tubule-specific NF-κB suppression was produced. In combination with *in vitro* studies using isolated primary proximal tubular cells we show that NF-κB plays an important role in controlling the recruitment of pro-inflammatory cells and in processes leading to apoptosis after hypoxia.

RESULTS

In vivo NF-κB Activity After Ischemia-Induced AKI

To assess the time course of NF-κB activation following IRI-induced AKI, we generated a transgenic mouse model expressing the luciferase gene under the control of NF-κB (*κ-Luc*). A gradually increased NF-κB activity was detected in *κ-Luc* mice after ischemia-induced AKI by measuring *in vivo* luciferase activity in the kidney (Figure 1A). NF-κB activation increased significantly 12 hours after ischemia, compared to sham-operated mice (Figure 1B). The peak of NF-κB activity was reached 2-3 days after ischemia and gradually decreased thereafter (Figure 1B). To define in which cell types NF-κB was activated, we stained uninephrectomized kidneys (as internal control) and kidneys after 24 hours of ischemia with an anti-phospho-S276-p65 (RelA) antibody to determine nuclear translocation of NF-κB. In kidneys subjected to ischemic injury followed by 24 hours of reperfusion, widespread nuclear phospho-p65 staining was observed in most tubular epithelial cells as well as in interstitial cells, whereas cells of the contralateral control kidney were not stained (Figure 1C, D).

Generation of a Genetic Mouse Model with Tubular Epithelial-Specific NF-κB Inhibition

To address the role of renal tubular NF-κB signaling in ischemic AKI, we generated a mouse model with tubular epithelial-specific NF-κB suppression using the Cre-loxP technology. First, we mated *Emx1-Cre* mice (http://www.informatics.jax.org/allele/MGI:1928281) with *Rosa 26 reporter (R26R)* mice to generate *Emx1Cre;R26R* reporter mice expressing β-galactosidase in cells with Cre-mediated recombination.[18] Immunofluorescence staining revealed β-galactosidase expression in proximal tubules labeled by aquaporin-1, in distal convoluted tubules positive for the sodium-chloride symporter solute carrier family 12 member 3, and in a subset of aquaporin-2-positive collecting duct cells (Figure 2A), but not in thick ascending limbs of Henle labeled by sodium-potassium-chloride cotransporter solute carrier family 12 member 2 or in the interstitium labeled by fibronectin and fibroblast specific protein (Supplemental Figure 1A). These data confirmed a specific activity of *Emx1-Cre* in renal tubular epithelium.

To suppress NF-κB activity in a tissue-specific manner, we used mice in which a floxed IκBαΔN (*loxP-IκBαΔN*) construct is expressed under control of the ubiquitously active *β-catenin* (*ctnnb1*) locus (Figure 2B).[19] The NF-κB super-repressor IκBαΔN lacks the N-terminal phosphorylation and ubiquitination sites of IκBα and is therefore rendered insensitive to degradation.[19] Offspring of

matings between *Emx1-Cre* and *loxP-IκBαΔN* mice bearing both the Emx1-driven *Cre* and one floxed *IκBαΔN* knock-in allele are referred to as *Emx1-ΔN* (Figure 2A). Immunoblot with IκBα-specific antibody on kidney lysates confirmed expression of IκBαΔN in *Emx1-ΔN* mice but not in controls (Figure 2C and Supplemental Figure 1B). To assess if the tubular expression of IκBαΔN reduces NF-κB activity in the kidney after ischemic AKI, kidney sections were stained with anti-phospho-S276-p65 antibody (Supplemental Figure 1C). Twenty-four hours after ischemia, kidneys of *Emx1-ΔN* mice showed significantly less nuclear P-p65 intensity in the cortex and in the medulla compared to kidneys of control mice (Figure 2D). A detailed analysis of NF-κB activity by P-p65 staining in the tubular nephron segments of injured control kidneys revealed a widespread nuclear P-p65 signal in segments of the nephron. In *Emx1-ΔN* mice, P-p65 signal was reduced in proximal tubules, distal tubules and partly in collecting ducts (Supplemental Figure 2A). Conversely, this difference was not evident in thick ascending limb of Henle's loop, where Cre activity is absent (Supplemental Figure 2B). Moreover, mRNA expression of IκBα (NFKBIA), a bona fide NF-κB target gene, was significantly reduced in *Emx1-ΔN* kidneys when compared to controls (Figure 2E).

Tubular Epithelial-Specific NF-κB Inhibition Attenuates Renal Damage after Ischemic AKI

To examine the effects of suppressed tubular NF-KB activity on overall renal damage, we performed ischemic AKI studies in *Emx1-ΔN* and control littermates. *Emx1-ΔN* mice showed a significantly lower elevation in serum creatinine levels 24 hours after ischemia compared to control mice (Figure 3A). In addition, renal mRNA levels and urinary protein levels of renal-damage marker, neutrophil gelatinase-associated lipocalin (NGAL), were significantly lower compared with control mice (Figure 3B, C). To assess the degree of tubular injury, kidney sections were stained and examined by an experienced renal pathologist unaware of genotype. These histological analyses clearly indicated an amelioration of cortical tubular ischemic injury in *Emx1-ΔN* mice as they presented less tubular necrosis and less tubular lumen occluded with cellular debris in the cortex (Figure 3D). In addition, the tubular injury score showed more intense damage in control mice compared with *Emx1-ΔN* mice (Figure 3E). Additional analysis of the S3 segments of the proximal tubule, which are most susceptible to ischemic injury, showed similar differences (Supplemental Figure 3A, B).

Reduced apoptosis and inflammation in *Emx1-ΔN* mice after Ischemic AKI

AKI is associated with increased infiltration of monocytes/macrophages and neutrophils, which contribute to the proinflammatory response in early AKI.[20] To detect neutrophil and macrophage

recruitment in the injured kidneys, we performed immunostaining and subsequently counted-labeled infiltrating cells in the outer medulla. Neutrophil and macrophage infiltration was significantly reduced 24 hours after ischemia in kidneys of *Emx1-ΔN* mice, compared with control mice (Figure 4A-D).

Renal tubular epithelial apoptosis can initiate reperfusion-induced inflammation and subsequent tissue injury.[21] As NF-κB plays an important role in apoptosis,[22] we aimed to determine the number of apoptotic tubular cells in the injured kidneys of control and *Emx1-ΔN* mice. Interestingly, compared to injured kidneys of control mice, kidneys of *Emx1-ΔN* mice showed a decreased rate of apoptosis as visualized by TUNEL labeling 24 hours after ischemia (Figure 5A). Quantification by direct counting of TUNEL-positive tubular cells confirmed this observation (Figure 5B).

The NF-κB-Dependent Gene Signature Following Ischemic AKI

To further define the effect of reduced tubular NF-κB signaling in the kidney following ischemic AKI, we performed microarray analysis on kidney samples, which were obtained from *Emx1-ΔN* or control mice 24 hours after induction of ischemia. Volcano plot revealed 240 genes differentially downregulated and 250 genes differentially upregulated in kidneys of Emx1-ΔN mice, compared to controls (fold change ≥ 1.2 and $P<0.05$, Figure 6A). Gene-set enrichment analysis[23] confirmed a highly significant overrepresentation of known NF-κB target genes within downregulated genes (Supplemental Figure 4A).

CD14 is a surface antigen preferentially expressed on monocytes/macrophages. The heterodimer, calprotectin (S100A8/A9), which has a wide plethora of intra- and extracellular functions colocalizes with Ly6G-positive neutrophils in AKI.[24] The mRNA levels of these proteins were significantly less expressed in injured kidneys of *Emx1-ΔN* mice compared to controls (Figure 6B). Moreover, gene expression of vascular cell adhesion molecule (VCAM) 1, as well as of the pro-inflammatory cytokines (interleukin (IL)-1β and IL-6) and chemokines (chemokine (C-X-C motif) ligand) (CXCL) 1 and CXCL2, were significantly reduced in injured kidneys of *Emx1-ΔN* mice compared with controls (Figure 6B).

For a more detailed investigation of the dynamics of the gene regulatory network governed by NF-κB, we analyzed gene expression at time points 6 hours, 24 hours, 48 hours, and 7 days after IRI-induced AKI in C57Bl/6J mice. We chose to restrict our analysis to differentially downregulated genes in Emx1-ΔN when compared to controls as they have shown enrichment for known NF-κB targets in Gene Set Enrichment Analysis (Supplemental Figure 4A). Most of these genes exhibited a transient peak expression at 6 hours after ischemia (Figure 6C, upper panel). However, when we performed a

more detailed analysis of the gene expression time courses using k-means clustering and merging of similar clusters a posteriori, we found distinct subsets of genes with markedly different expression patterns (see Methods for a detailed description of the clustering analysis). The largest gene groups identified by this analysis comprised two gene sets, which we designated clusters 1 and 2 (Figure 6C, lower panels; see Supplemental Tables 2 and 3 for a full list of genes, clusters, and ontology terms). Cluster 1 peaked at 6 hours following AKI and quickly returned to baseline thereafter. This cluster contained genes mostly involved in apoptosis, cell death, and immune cell chemotaxis. Cluster 2 displayed a delayed expression peak at 7 days and contained genes responsible for endocytosis, immune cell apoptosis, epithelial morphogenesis and wound healing. Hence, these findings suggest different time-dependent functions for NF-κB signaling following ischemic AKI in the kidney. Differentially expressed genes in the NF-κB signaling pathway from Kyoto Encyclopedia of Genes and Genomes (KEGG) are visualized on Supplemental Figure 4B.

NF-κB Inhibition Leads to Reduced Apoptosis and Reduced Chemokine Expression Upon Cobalt Chloride ($CoCl_2$) treatment in Primary Proximal Tubular Cells

To differentiate between direct and indirect effects of tubular NF-κB signaling, we isolated proximal tubular epithelial cells from *IκBαΔN*^{ubi} mice and control mice. The stabilization of hypoxia-inducible factor (HIF)1α protein is a hallmark of hypoxia. To mimic hypoxia *in vitro*, cells were exposed to HIF1α stabilizing agent $CoCl_2$ in a low glucose medium for 24 hours. We subsequently determined the percentage of apoptotic cells using Hoechst staining followed by fluorescent microscopy analyses (Figure 7A). Tubular cells expressing the NF-κB super-repressor IκBαΔN showed reduced apoptosis compared with control cells (Figure 7B). The mRNA expression of the HIF1α target gene vascular endothelial growth factor (VEGF) was upregulated by $CoCl_2$ treatment in both groups (Figure 7C). CXCL1 and CXCL2 were only induced in control proximal tubular cells after $CoCl_2$ treatment but not in cells expressing IκBαΔN (Figure 7D). Together, these data support a direct role of NF-κB signaling in tubular epithelial apoptosis and in the control of chemotactic cytokine expression by proximal tubules upon HIF1α stabilization.

DISCUSSION

We demonstrate that inhibiting NF-κB signaling in renal tubular epithelium reduces tubular injury, apoptosis, necrosis, and accumulation of interstitial inflammatory cells, which consequently results in ameliorated kidney damage after ischemic AKI induction. The treatment of primary proximal tubular cell cultures with hypoxia-mimetic agent $CoCl_2$ further confirmed that reduced NF-κB activity *per se* reduces apoptosis and expression of certain chemokines. Previous work already implicated endothelial cell-specific suppression of NF-κB activity in the attenuation of hypertension-induced renal damage despite high blood pressure.[25] Although endothelial NF-κB inhibition did not affect the development of hypertension, it diminished the upregulation of several proinflammatory NF-κB target genes including VCAM-1 and ICAM-1 and reduced renal inflammation and tubular damage. This state-of-affairs suggests that renal damage is, at least in part, dependent on NF-κB activity in vascular endothelial and tubular epithelial cells. NF-κB activity in these two compartments may be required for production of cytokines and chemokines and recruitment of immune cells.

For the present study, we generated mice with suppressed NF-κB activity in the tubular epithelium (*Emx1-ΔN*). To analyze the time course of NF-κB activation during ischemic AKI, for the first time we employed a luciferase-dependent *in vivo* imaging technique using an NF-κB reporter mouse model (*κ-Luc*). Twelve hours after ischemic AKI induction, *κ-Luc* mice revealed a significant increase of NF-κB activity which lasted 5 days before it returned to base levels. Unfortunately, this technique does not allow us to differentiate between NF-κB activity derived from kidney cells or from infiltrating immune cells. However, phospho-p65 immunostaining showed an almost global increase of nuclear NF-κB activity in all renal compartments 24 hours following ischemic AKI induction, which suggests that a considerable amount, if not the majority of NF-κB-induced luciferase activity stems from kidney cells.

Consistent with previous studies using global NF-κB silencing in different AKI models by injecting p105 or RelB silencing RNAs into the tail vein,[10, 26] or by injecting NF-κB decoy oligodeoxynucleotides directly into the renal artery,[8, 9, 11] we also observed reduced infiltration of neutrophils and macrophages in the injured kidneys of *Emx1-ΔN* mice. Neutrophils and monocytes/macrophages respond rapidly to renal injury and play an important role in the deterioration of renal functions in AKI.[27] However, the role of different macrophage subtypes in AKI and in subsequent repair and regeneration is currently explored.[28] In our AKI model the mRNA levels of a classically activated macrophage marker, inducible nitric oxide synthase, and alternatively activated macrophage marker, interferon regulatory factor 4, were not significantly reduced in injured kidneys of mice with tubular IκBαΔN expression (Data not shown).

Surprisingly, after ischemia we found less apoptosis in *Emx1-ΔN* mice compared with control mice. Although NF-κB is generally regarded as anti-apoptotic, in particular contexts and especially in response to cellular stress NF-κB can promote apoptosis.[29] In line with this explanation, in proximal tubular cell cultures overexpressing IκBαΔN we found reduced apoptosis following hypoxia-mimetic $CoCl_2$ treatment. Nevertheless, these results should be interpreted with caution. $CoCl_2$ does not induce hypoxia, but instead activates hypoxia-mediated signaling pathways under normoxia by stabilizing the cytosolic HIF1α. Despite the pro-apoptotic effect of $CoCl_2$ in our model, HIF1α can also exert anti-apoptotic effects[30] and thus it may interfere with potential anti-apoptotic effects of NF-κB suppression. Complicating issues, IκBα has been reported to be a target of the HIF1α-regulating hydroxylase factor inhibiting HIF.[31] Depite these caveats, the finding of reduced apoptosis in isolated proximal tubular cells overexpressing IκBαΔN suggests that the reduced apoptosis rate represents a cell-autonomous effect of suppressed tubular NF-κB activity in renal tubules, which is independent from the tissue microenvironment and from inflammatory cell infiltrates. Inhibition of apoptosis induced by ischemia-reperfusion was previously shown to prevent inflammation.[21] Therefore, the reduced apoptosis observed in *Emx1-ΔN* may also contribute to the reduced immune cell infiltration seen in these mice after ischemia.

NF-κB regulates the expression of numerous genes, including cytokines/chemokines, cell adhesion molecules and stress response genes (http://www.bu.edu/nf-kb/). In the context of ischemic renal injury, several NF-κB-dependent target genes were also expressed in tubular cells.[27, 32] Indeed, following induction of ischemic AKI kidneys of *Emx1-ΔN* mice showed significantly reduced expression of the murine homologues of human IL-8, CXCL1 and CXCL2, and IL-1β compared with control mice, which was verified in an *in vitro* model of chemical hypoxia in IκBαΔN-overexpressing primary proximal tubular cell cultures. This state-of-affairs indicates that tubular cells upregulate these molecules during ischemia and that their expression is dependent on NF-κB activity. A functional role for CXCL1 and 2 in AKI was further confirmed by a study demonstrating that treatment with an inhibitor of the CXCL1/CXCL2 receptor or with neutralizing antibodies against CXCL1 or CXCL2 during renal ischemia blocked interstitial neutrophil infiltration, reduced renal damage, and improved survival.[33, 34] In addition, expression of VCAM1, which is induced on vascular endothelial cells by cytokine,[35] was also significantly reduced in AKI-injured *Emx1-ΔN* kidneys, suggesting a crosstalk between tubular and endothelial cells. Supporting this notion, in the study by Henke and colleagues in which NF-κB was endothelial cell-specifically inhibited, tubular epithelial damage was also ameliorated.[25]

Interestingly, a more detailed time-course-dependent comparison of differentially expressed genes between *Emx1-ΔN* and control kidneys revealed sets of genes, which could be assigned to distinct

time-dependent functions. We show here that NF-κB is involved in regulating functional target gene programs including cell death, which peaks approximately 6 hours after AKI induction, while repair and morphogenesis pathways peak 7 days after ischemia. In summary, this finding suggests that persistent NF-κB activity results in time-dependent physiological changes in the kidney, which plays an important role in the development of AKI.

NF-κB was initially identified as a transcription factor bound to the enhancer of the immunoglobulin kappa light chain gene in B lymphocytes.[36] The omnipotence of NF-κB soon became clear, and many renal diseases have also been associated with impaired NF-κB activity.[7, 37] Nevertheless, most of the evidence that links NF-κB activation to human and experimental kidney disease is descriptive, based on experiments with cell lines or performed in a way in which the effects of NF-κB modulation cannot be attributed to specific kidney cell types, which makes the physiological understanding of NF-κB in renal diseases difficult. However, we analyzed a mouse model with specific NF-κB suppression in the tubular epithelium. Using this mouse model we shed light on the importance of the tubular epithelium in the development of ischemic AKI. Our results may also help to understand the role of tubular NF-κB signaling in other renal diseases and to develop novel targeted drug treatments.

CONCISE METHODS

Mice

Transgenic mice expressing the luciferase gene under the control of NF-κB (*κ-Luc, B6-Tg(κ-Luc)1Gr/Rsu*) carry 3 NF-κB DNA binding elements from the Igκ light chain enhancer hooked to the luciferase gene. The luciferase reporter mice were generated based on the κ-Gal construct published earlier[38] to non-invasively determine the *in vivo* pattern of NF-κB activity after induction of ischemia. Albino C57BL/6 mice were used to avoid quenching of luminescence.

Mice with tubular cell–restricted NF-κB suppression were generated by mating *Emx1-Cre* knock-in mice (*Emx1*$^{tm1.1(cre)Ito}$ a generous gift from Shigeyoshi Itohara, RIKEN Brain Science Institute, 2-1 Hirosawa, Wako City) with *floxed IκBαΔN* (*loxP-IκBαΔN, B6.129P2-ctnnb1*$^{tm(NFKBIAΔNfl/fl)Rsu}$) mice in which the cDNA of the human NF-κB super-repressor *IκBαΔN* was knocked into the *β-catenin* (*Ctnnb1*) locus (see Figure 2A).[19] Offspring that did not express IκBαΔN (wildtype, *Emx1-Cre* or *loxP-IκBαΔN* mice) were used as controls. *Emx1-ΔN* mice developed normally, without any obvious phenotype. Kidneys of mice ubiquitously expressing the human NF-κB super-repressor IκBαΔN (*IκBαΔN*^{ubi}; *B6.129P2-ctnnb1*$^{tm(NFKBIAΔN)1Rsu}$) were used as positive control for Western blot analysis and for *in vitro* studies.[19]

Emx1 promoter activity in the kidney was assessed by mating *Emx1-Cre* knock-in mice with Rosa 26 reporter (*R26R*, *B6;129S-Gtrosa26*^{tm1Sor}) mice.[18] *Emx1-Cre*-mediated activation of β-galactosidase in the various kidney compartments was determined by using specific anti-β-galactosidase antibodies (detailed under Immunofluorescence).

The Berlin Animal Review Board approved all protocols that were conducted to National Institute of Health Guide for the Care and Use of Laboratory Animals standards.

***In Vivo* Renal Ischemia-Reperfusion Model**

Male mice between 12-15 weeks were used. Anesthesia was performed with isoflurane (2.3%) in air (350 ml/min). Each mouse was operated separately to ensure similar exposure to isoflurane (33±3 minutes, mean±SD). A temperature controller with heating pad (TCAT-2, Physitemp Instruments) was used to keep body temperature stable at 37°C during surgery in order to induce warm ischemia. Rectal body temperature was continuously monitored using a sensor based on thermistors and values were recorded at different time points. Ischemia was induced after right-sided uninephrectomy by clipping the pedicles of the remaining left kidney for 17.5 minutes with non-traumatic aneurysm clip (FE690K, Aesculap). Reperfusion was confirmed visually. After surgery, mice had free access to water and chow. We applied body-warm sterile physiological saline solution and

analgesia with tramadol (1 mg/kg) for every mouse. Sham surgery was performed in a similar manner, except for clamping the renal vessels. Mice with bleeding after uninephrectomy, with incomplete renal reperfusion after ischemia, with excessive exposure of isoflurane of any reason, with significant temperature fluctuation during ischemia or with signs for infection after 24 hours were immediately killed and were not used for further analysis. After 24 hours of reperfusion mice were sacrificed, and kidney and blood was collected for further analysis. The kidneys were divided into three. One third of the kidney was placed in optimum cutting temperature (OCT) compound for immunohistochemistry, one third was immersed in 4% phosphate-buffered saline (PBS)-buffered formalin for histology and the rest was snap-frozen in liquid nitrogen for quantitative real-time (qRT)-PCR.

***In Vivo* Bioluminescence imaging of NF-κB Activity during Reperfusion**

Two days before bioluminescence imaging, mice were shaven dorsally at the sites of the kidneys to prevent any quenching of the bioluminescent signal by the fur. *κ-Luc* reporter mice were anesthetized with 2.5% isoflurane and injected subcutaneously with 1.5 mg D-luciferin (VivoGlo, Promega) in 100 µl PBS (pH 7.0). Whole-body image was acquired after an exposure time of 60 seconds using an In Vivo Imaging System (IVIS Spectrum, PerkinElmer). Mice were measured at different time points after ischemia as depicted in Figure 1A. To obtain the luciferin kinetics, every 2 minutes an image was acquired subsequently 10 times after D-luciferin injection. From the luciferin kinetics, the measurements showing maximal radiance were used for quantification. Using Living Image Software v4.2 (Caliper LifeSciences) the bioluminescent signal was quantified. Data are presented in physical units of radiance in photons/sec/cm^2/steradian.

Serum and Urine Measurements

Blood samples were taken from left ventricle at termination. After clotting on room temperature for at least 15 minutes blood was centrifuged at 2,000×g for 10 minutes to obtain serum. Automated techniques were used to measure serum creatinine (Beckman Analyzer, Beckman Instruments). To assess basal laboratory parameters 100 µL blood was taken from facial region and parameters were measured using an i-STAT system with Chem8+ cartridges (Abbott). Urine sodium, creatinine was measured in 24-hour collected urine by Labor 28 (Berlin, Germany). Urine osmolarity of 24-hour collected urine was measured using freezing point depression (Advance Instruments).

qRT-PCR

Total RNA from snap-frozen kidneys and proximal tubular cells were isolated using RNeasy RNA isolation kit (Qiagen). RNA concentration and quality was measured by NanoDrop-1000 spectrophotometer (Thermo Fisher Scientific). Two micrograms of RNA were used for cDNA transcription (Applied Biosystems). Quantitative analysis of target mRNA expression was performed with qRT-PCR using the relative standard curve method. TaqMan and SYBR green analysis was conducted using an Applied Biosystems 7500 Sequence Detector (Applied Biosystems). The expression levels were normalized to 18s. Biotez synthesized the primers and the sequences are provided in the in online supplement (Supplemental Table 1).

Microarray and K-means clustering

Total RNA isolated from kidneys as mentioned before were used for synthesis of cRNA by Illumina TotalPrep RNA Amplification kit (#AMIL1791, Thermo Fischer Scientific). The Illumina platform MouseWG-6 v2.0 Expression BeadChip Kit was used that assays more than 45,000 transcripts. Kits were used according to manufacturer's instruction.

K-means clustering has been performed on the normalized gene expression data over time. That is, for each gene, we had 5 expression values corresponding to 0, 6, 24, 48 hours and 7 days. These values were normalized for each single gene such that the maximum over time corresponded to 1 and the minimum to 0. These operations were performed for all genes separately. The normalized expression vectors were then clustered using k-means. For a k=20, 80% of the data's variance over time could be explained, thus, this k was chosen for clustering. The strongest clusters were then more closely investigated and were merged if they exhibited comparable patterns over time. These analyses gave 3 main clusters presented in Figure 6C, lower panels.

Western Blot

Kidney tissues were harvested from mice with different genotypes and were lysed with RIPA buffer (Sigma) supplemented with Complete Mini protease inhibitor (Roche), 1 mM phenylmethylsulfonyl fluoride (PMSF), Phosphatase inhibitor cocktail 3 (Sigma) and were homogenized using a Precellys 24 homogenizator (Peqlab). Fifty µg protein samples were separated by 12% SDS-PAGE. After semi-dry transfer, non-specific binding sites of the nitrocellulose membrane were blocked with 5% non-fat milk in Tris-buffered saline containing 0.1% Tween (TBS-T). After that the membrane was incubated with the primary antibody against IκBα (1:200; sc-371 C-21, Santa Cruz). Secondary antibody was

from LI-COR Biosciences (anti-rabbit, 1:5000). Images were acquired by Odyssey infrared imaging system (LI-COR Biosciences).

Urine was collected from the bladder of mice subjected to ischemia 24 hours following surgery. Ten µl of urine were mixed with 4× non-reducing Nu-Page loading buffer (Invitrogen) and loaded on NuPage 4-12% Bis-Tris gel (Invitrogen). Afterwards, the proteins were blotted on a polyvinylidene fluoride membrane, which was further blocked in 5% non-fat milk in TBST for 1 hour at room temperature and then incubated overnight at 4°C with polyclonal anti-NGAL primary antibody (1:2000; #AF-1857, R&D Systems). Urinary NGAL was detected with horseradish peroxidase-conjugated secondary antibody (1:5000; #705-035-147, Jackson ImmunoResearch.) and chemiluminescent reagent (Super Signal-West Pico, Thermo Scientific). Known amounts of recombinant mouse NGAL protein (#1857-LC, R&D) were used as standards.

Microscopy

Histology

We stained formalin-fixed, paraffin-embedded sections (2 µm) of kidneys with Masson's trichrome stain using standard protocols. The severity of tubular injury was assessed by a renal pathologist blinded to the genotype of the mice. Tubular necrosis was evaluated in a semi-quantitative manner by determining the percentage of tubules in the cortex in which epithelial necrosis, loss of the brush border, cast formation, and tubular dilation was observed. A five-point scale was used: 0, normal kidney; 1: 1 to 25%; 2: 25 to 50%; 3: 50 to 75%; and 4, 75 to 100% tubular necrosis.

Immunohistochemistry

Formalin-fixed, paraffin-embedded 2 µm thick sections were stained for S276 specific phosphorylated P-p65 (1:200; ab106129, Abcam). For visualization the EnVision+ Kit (Dako) was used according to manufacturer's instruction as well as hematoxylin as a counterstain.

Immunofluorescence

For *R26R* mice 14 µm, in all other cases 5 µm thick cryosections were post-fixed in ice-cold acetone, air-dried, rehydrated and blocked with 10% normal donkey serum (Jackson ImmunoResearch) for 30 min. Then sections were incubated overnight at 4°C with the following primary antibodies: rat anti-F4/80 (1:200; MCA497; AbD Serotec), rat anti-Ly-6B.2 (Gr1) (1:300; MCA771G; AbD Serotec), rabbit anti-aquaporin-1 (1:300; AB2219, Millipore), rabbit anti-sodium-chloride symporter (1:500; AB3553;

Millipore), rabbit anti-aquaporin-2 (1:500; ab15116, Abcam), goat anti-aquaporin-2 (1:200, sc-9882; Santa Cruz Biotechnologies), mouse anti-FSP (1:250; F4771, Sigma), rabbit anti-fibronectin, (1:500; F3648, Sigma), rabbit anti-sodium-potassium-chloride cotransporter 2 (1:1000; a gift from Sebastian Bachmann, Charité Berlin), chicken anti-β-galactosidase (1:50; ab9361; Abcam) and rabbit anti-S276 P-p65 (1:200; ab106129, Abcam). All incubations were performed in a humid chamber. For fluorescence visualization of bound primary antibodies, sections were further incubated with appropriate Cy3- or Alexa 488-conjugated secondary antibodies (1:500; Jackson ImmunoResearch) for 1 h in a humid chamber at room temperature.

TUNEL Assay

Formalin-fixed, paraffin-embedded 2 µm thick sections were labeled after pepsin-treatment with TMR In Situ Cell Death Detection Kit (Roche) according to the instructions of the manufacturer. Slides were counterstained with the nuclear dye 4',6-diamidino-2-phenylindole (DAPI, Sigma) in order to visualize cell nuclei. Percentage of TUNEL-positive tubular cells was determined in the outer medulla by Zeiss Axio Imager.M2 fluorescence upright microscope using 63× Plan-Apochromat immersion oil objective.

Apoptosis Assay

Apoptosis assay was performed as described previously.[39] Briefly, primary proximal tubular cells were plated onto poly-L-lysine coated glass coverslips and were cultured overnight. 24 hours later the medium was exchanged to fresh DMEM (Sigma) containing 1000mg/l glucose, 10% fetal calf serum (Biochrom) 10%, 100 IU/ml penicillin (Sigma) and 100 µg/ml streptomycin (Sigma). Cells were treated with 300 µM $CoCl_2$ (Sigma) or kept untreated as described under the section "HIF1α Stabilization in Primary Proximal Tubular Cell". After 24 hours cells were fixed with 4% paraformaldehyde-containing PBS. Cell nuclei were stained with Hoechst 33342 fluorescent DNA-dye. Nuclear morphology of the samples was scored. At least 100-150 cell nuclei/sample were analyzed on randomly chosen view fields according to typical apoptotic nuclear morphology by Zeiss Axio Imager.M2 fluorescence upright microscope using 63× Plan-Apochromat immersion oil objective.

Quantitative Digital Image Analyses

All images were taken using a Zeiss Axioplan-2 imaging microscope with the computer program AxioVision 4.8 (Zeiss). Intensity of the staining of P-p65 was calculated as follows; for each analyzed

picture, 10 randomly chosen nuclei were cut out manually, the rest of the image was deleted. Every pixel was then transformed into an RGB (red, green, blue) number triplet and normalized to length 1 as we did not wish to measure brightness. The red channel count (RCC), as presented in the figures, is the value derived by # (pixels with entry >0.699 of the red channel in RGB after normalization)/#(pixels in the cut image). The threshold was derived from pixels of clear P-p65 staining and the RCC is independent of image resolution. F4/80-positive and Gr1-positive cells were counted in 20 non-overlapping view fields in the cortex and the outer medulla at ×630 magnification. TUNEL-positive epithelial cells were counted at ×630 magnification in 5 non-overlapping outer medulla view fields and the numbers of positive cells were divided by the total cell number of that view field.

Primary Proximal Tubular Cell Isolation

Cells were obtained and cultured as described previously.[40] Briefly, kidneys of *IκBαΔN*^{ubi} and littermate control mice aged 10-12 weeks were euthanized by overdose of isoflurane and flushed with 10 ml ice-cold PBS (Sigma) through left ventricle. Renal cortices were dissected visually and minced into small pieces. The fragments were transferred through two layers of stainless steel sieves (pore size 125 µm and 106 µm; Linker). Tubular fragments caught by the 106 µm sieve were flushed in the reverse direction with PBS and centrifuged for 5 minutes at 170×g, washed, and then resuspended into the appropriate amount of culture medium: 1:1 DMEM/F12 (D 8437; Sigma) supplemented with fetal calf serum (FCS) 10%, penicillin 100 IU/ml and streptomycin 100 µg/ml buffered to pH 7.4. Plate was incubated in a standard humidified incubator equipped with 5% CO_2. Medium was changed two days later and maintained every other day until the monolayer of cells reached 90% confluence; at this time over 90% of the isolated cells were megalin-positive (sheep-anti-LRP2 antibody (1:10000) was a gift from Prof. Thomas Willnow; secondary antibody was donkey anti-sheep Alexa 555 (1:2000; Thermo Fisher Scientific)).

HIF1α Stabilization in Primary Proximal Tubular Cell

Primary proximal tubular cells isolated from *IκBαΔN*^{ubi} and littermate control mice were treated with 300 µm $CoCl_2$ or left untreated in a low-glucose DMEM medium (D6046, Sigma) for 24 hours to stabilize HIF1α. Low glucose medium was used because it is known that cell death in proximal tubular cell cultures is HIF1α-dependent only when glucose availability is limited.[41] Optimal concentration of $CoCl_2$ and length of treatment were determined by preliminary experiments. After 24 hours medium was removed and cells were harvested for further analysis.

Statistics

Statistical analysis was performed using GraphPad 5.04 (GraphPad Software) and SPSS 13.0 (SPSS) software. Normality of the data was tested by Kolmogorov-Smirnov test. To test the presence of an outlier Grubbs' test was used. Mann-Whitney U test (data with non-normal distribution) or unpaired t-test (data with normal distribution) was used in case of 2 groups as stated in figure legends. In case of more than 2 groups data were analyzed by one-way ANOVA using Newman-Keuls post-hoc test. Data are presented as mean±SEM. P values <0.05 were considered as statistically significant.

ACKNOWLEDGMENTS

This work was supported by the Deutsche Forschungsgemeinschaft (DFG) (FOR 1368 to R. S-U., K. S-O. and D. N. M.). K. S.-O. is supported by the Urological Research Foundation. We thank Gabriele N'diaye, Dr. Sabine Bartel, May-Britt Köhler, Sarah Ugowski and Petra Berkefeld for their excellent technical assistance.

Disclosures: None.

REFERENCES

1. Mehta, RL, Cerda, J, Burdmann, EA, Tonelli, M, Garcia-Garcia, G, Jha, V, Susantitaphong, P, Rocco, M, Vanholder, R, Sever, MS, Cruz, D, Jaber, B, Lameire, NH, Lombardi, R, Lewington, A, Feehally, J, Finkelstein, F, Levin, N, Pannu, N, Thomas, B, Aronoff-Spencer, E, Remuzzi, G: International Society of Nephrology's 0by25 initiative for acute kidney injury (zero preventable deaths by 2025): a human rights case for nephrology. *Lancet*, 385: 2616–2643, 2015
2. Bellomo, R, Kellum, JA, Ronco, C: Acute kidney injury. *Lancet,* 380**:** 756-766, 2012
3. Glodowski, SD, Wagener, G: New insights into the mechanisms of acute kidney injury in the intensive care unit. *J Clin Anesth,* 27**:** 175-180, 2015
4. Ghosh, S, Hayden, MS: Celebrating 25 years of NF-kappaB research. *Immunol Rev,* 246**:** 5-13, 2012.
5. Hinz, M, Arslan, SC, Scheidereit, C: It takes two to tango: IkappaBs, the multifunctional partners of NF-kappaB. *Immunol Rev,* 246**:** 59-76, 2012
6. Natoli, G: NF-kappaB and chromatin: ten years on the path from basic mechanisms to candidate drugs. *Immunol Rev,* 246**:** 183-192, 2012
7. Guijarro, C, Egido, J: Transcription factor-kappa B (NF-kappa B) and renal disease. *Kidney Int,* 59**:** 415-424, 2001
8. Vos, IH, Govers, R, Grone, HJ, Kleij, L, Schurink, M, De Weger, RA, Goldschmeding, R, Rabelink, TJ: NFkappaB decoy oligodeoxynucleotides reduce monocyte infiltration in renal allografts. *FASEB J,* 14**:** 815-822, 2000
9. Cao, CC, Ding, XQ, Ou, ZL, Liu, CF, Li, P, Wang, L, Zhu, CF: In vivo transfection of NF-kappaB decoy oligodeoxynucleotides attenuate renal ischemia/reperfusion injury in rats. *Kidney Int,* 65**:** 834-845, 2004
10. Feng, B, Chen, G, Zheng, X, Sun, H, Zhang, X, Zhang, ZX, Xiang, Y, Ichim, TE, Garcia, B, Luke, P, Jevnikar, AM, Min, WP: Small interfering RNA targeting RelB protects against renal ischemia-reperfusion injury. *Transplantation,* 87**:** 1283-1289, 2009
11. Wan, X, Fan, L, Hu, B, Yang, J, Li, X, Chen, X, Cao, C: Small interfering RNA targeting IKKbeta prevents renal ischemia-reperfusion injury in rats. *Am J Physiol Renal Physiol,* 300**:** F857-F863, 2011
12. Wullaert, A, Bonnet, MC, Pasparakis, M: NF-kappaB in the regulation of epithelial homeostasis and inflammation. *Cell Res,* 21**:** 146-158, 2011
13. Lentsch, AB: Activation and function of hepatocyte NF-kappaB in postischemic liver injury. *Hepatology,* 42**:** 216-218, 2005
14. Neurath, MF, Pettersson, S, Meyer zum Buschenfelde, KH, Strober, W: Local administration of antisense phosphorothioate oligonucleotides to the p65 subunit of NF-kappa B abrogates established experimental colitis in mice. *Nat Med,* 2**:** 998-1004, 1996
15. Shibata, W, Maeda, S, Hikiba, Y, Yanai, A, Ohmae, T, Sakamoto, K, Nakagawa, H, Ogura, K, Omata, M: Cutting edge: The IkappaB kinase (IKK) inhibitor, NEMO-binding domain peptide, blocks inflammatory injury in murine colitis. *J Immunol,* 179**:** 2681-2685, 2007
16. Nenci, A, Becker, C, Wullaert, A, Gareus, R, van Loo, G, Danese, S, Huth, M, Nikolaev, A, Neufert, C, Madison, B, Gumucio, D, Neurath, MF, Pasparakis, M: Epithelial NEMO links innate immunity to chronic intestinal inflammation. *Nature,* 446**:** 557-561, 2007
17. van Hogerlinden, M, Rozell, BL, Ahrlund-Richter, L, Toftgard, R: Squamous cell carcinomas and increased apoptosis in skin with inhibited Rel/nuclear factor-kappaB signaling. *Cancer Res,* 59**:** 3299-3303, 1999
18. Soriano, P: Generalized lacZ expression with the ROSA26 Cre reporter strain. *Nat Genet,* 21**:** 70-71, 1999
19. Schmidt-Ullrich, R, Aebischer, T, Hulsken, J, Birchmeier, W, Klemm, U, Scheidereit, C: Requirement of NF-kappaB/Rel for the development of hair follicles and other epidermal appendices. *Development,* 128**:** 3843-3853, 2001

20. Bonventre, JV, Yang, L: Cellular pathophysiology of ischemic acute kidney injury. *J Clin Invest,* 121**:** 4210-4221, 2011
21. Daemen, MA, van 't Veer, C, Denecker, G, Heemskerk, VH, Wolfs, TG, Clauss, M, Vandenabeele, P, Buurman, WA: Inhibition of apoptosis induced by ischemia-reperfusion prevents inflammation. *J Clin Invest,* 104**:** 541-549, 1999
22. Beg, AA, Sha, WC, Bronson, RT, Ghosh, S, Baltimore, D: Embryonic lethality and liver degeneration in mice lacking the RelA component of NF-kappa B. *Nature,* 376**:** 167-170, 1995.
23. Subramanian, A, Tamayo, P, Mootha, VK, Mukherjee, S, Ebert, BL, Gillette, MA, Paulovich, A, Pomeroy, SL, Golub, TR, Lander, ES, Mesirov, JP: Gene set enrichment analysis: a knowledge-based approach for interpreting genome-wide expression profiles. *Proc Natl Acad Sci U S A,* 102**:** 15545-15550, 2005
24. Dessing, MC, Tammaro, A, Pulskens, WP, Teske, GJ, Butter, LM, Claessen, N, van Eijk, M, van der Poll, T, Vogl, T, Roth, J, Florquin, S, Leemans, JC: The calcium-binding protein complex S100A8/A9 has a crucial role in controlling macrophage-mediated renal repair following ischemia/reperfusion. *Kidney Int,* 87**:** 85-94, 2015
25. Henke, N, Schmidt-Ullrich, R, Dechend, R, Park, JK, Qadri, F, Wellner, M, Obst, M, Gross, V, Dietz, R, Luft, FC, Scheidereit, C, Muller, DN: Vascular endothelial cell-specific NF-kappaB suppression attenuates hypertension-induced renal damage. *Circ Res,* 101**:** 268-276, 2007
26. Hocherl, K, Schmidt, C, Kurt, B, Bucher, M: Inhibition of NF-kappaB ameliorates sepsis-induced downregulation of aquaporin-2/V2 receptor expression and acute renal failure in vivo. *Am J Physiol Renal Physiol,* 298**:** F196-F204, 2010
27. Kinsey, GR, Li, L, Okusa, MD: Inflammation in acute kidney injury. *Nephron Exp Nephrol,* 109**:** e102-e107, 2008
28. Kinsey, GR: Macrophage dynamics in AKI to CKD progression. *J Am Soc Nephrol,* 25**:** 209-211, 2014
29. Kucharczak, J, Simmons, MJ, Fan, Y, Gelinas, C: To be, or not to be: NF-kappaB is the answer--role of Rel/NF-kappaB in the regulation of apoptosis. *Oncogene,* 22**:** 8961-8982, 2003
30. Yu, EZ, Li, YY, Liu, XH, Kagan, E, McCarron, RM: Antiapoptotic action of hypoxia-inducible factor-1 alpha in human endothelial cells. *Lab Invest,* 84**:** 553-561, 2004
31. Cockman, ME, Lancaster, DE, Stolze, IP, Hewitson, KS, McDonough, MA, Coleman, ML, Coles, CH, Yu, X, Hay, RT, Ley, SC, Pugh, CW, Oldham, NJ, Masson, N, Schofield, CJ, Ratcliffe, PJ: Posttranslational hydroxylation of ankyrin repeats in IkappaB proteins by the hypoxia-inducible factor (HIF) asparaginyl hydroxylase, factor inhibiting HIF (FIH). *Proc Natl Acad Sci U S A,* 103**:** 14767-14772, 2006
32. Bonventre, JV, Zuk, A: Ischemic acute renal failure: an inflammatory disease? *Kidney Int,* 66**:** 480-485, 2004
33. Cugini, D, Azzollini, N, Gagliardini, E, Cassis, P, Bertini, R, Colotta, F, Noris, M, Remuzzi, G, Benigni, A: Inhibition of the chemokine receptor CXCR2 prevents kidney graft function deterioration due to ischemia/reperfusion. *Kidney Int,* 67**:** 1753-1761, 2005
34. Miura, M, Fu, X, Zhang, QW, Remick, DG, Fairchild, RL: Neutralization of Gro alpha and macrophage inflammatory protein-2 attenuates renal ischemia/reperfusion injury. *Am J Pathol,* 159**:** 2137-2145, 2001
35. Osborn, L, Hession, C, Tizard, R, Vassallo, C, Luhowskyj, S, Chi-Rosso, G, Lobb, R: Direct expression cloning of vascular cell adhesion molecule 1, a cytokine-induced endothelial protein that binds to lymphocytes. *Cell,* 59**:** 1203-1211, 1989
36. Sen, R, Baltimore, D: Inducibility of kappa immunoglobulin enhancer-binding protein Nf-kappa B by a posttranslational mechanism. *Cell,* 47**:** 921-928, 1986
37. Sanz, AB, Sanchez-Nino, MD, Ramos, AM, Moreno, JA, Santamaria, B, Ruiz-Ortega, M, Egido, J, Ortiz, A: NF-kappaB in renal inflammation. *J Am Soc Nephrol,* 21**:** 1254-1262, 2010
38. Schmidt-Ullrich, R, Memet, S, Lilienbaum, A, Feuillard, J, Raphael, M, Israel, A: NF-kappaB activity in transgenic mice: developmental regulation and tissue specificity. *Development,* 122**:** 2117-2128, 1996

39. Balogh, A, Nemeth, M, Koloszar, I, Marko, L, Przybyl, L, Jinno, K, Szigeti, C, Heffer, M, Gebhardt, M, Szeberenyi, J, Muller, DN, Setalo, G, Jr., Pap, M: Overexpression of CREB protein protects from tunicamycin-induced apoptosis in various rat cell types. *Apoptosis,* 19**:** 1080-1098, 2014
40. Zhang, JD, Patel, MB, Griffiths, R, Dolber, PC, Ruiz, P, Sparks, MA, Stegbauer, J, Jin, H, Gomez, JA, Buckley, AF, Lefler, WS, Chen, D, Crowley, SD: Type 1 angiotensin receptors on macrophages ameliorate IL-1 receptor-mediated kidney fibrosis. *J Clin Invest,* 124**:** 2198-2203, 2014
41. Biju, MP, Akai, Y, Shrimanker, N, Haase, VH: Protection of HIF-1-deficient primary renal tubular epithelial cells from hypoxia-induced cell death is glucose dependent. *Am J Physiol Renal Physiol,* 289**:** F1217-F1226, 2005

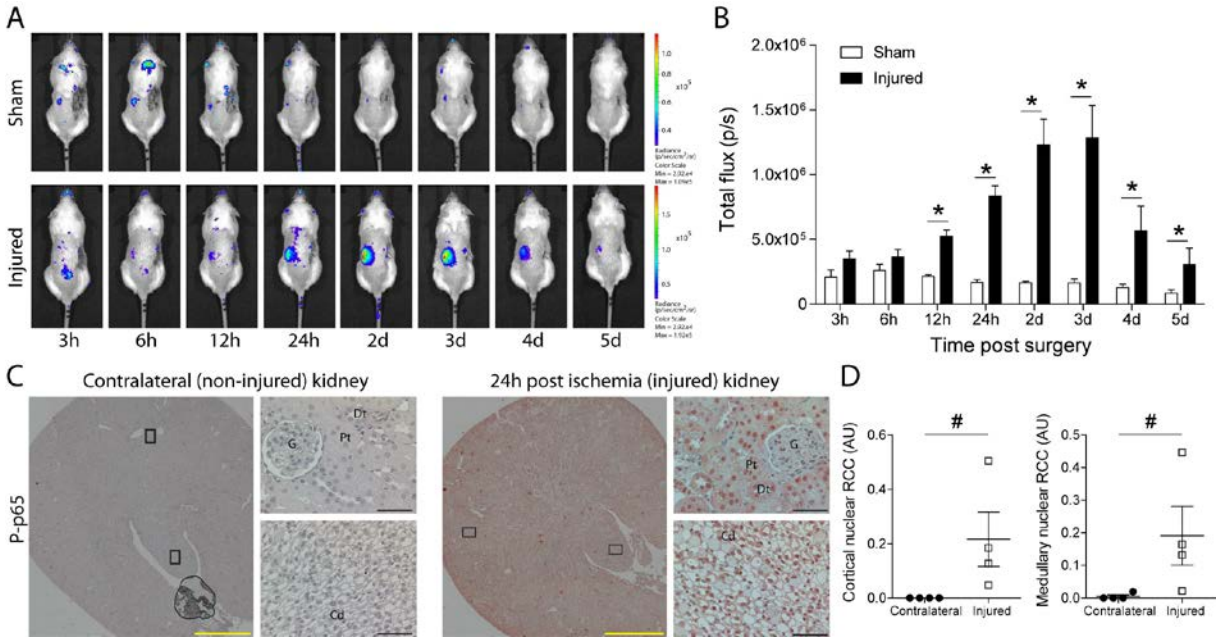

Figure 1. Time course and localization of NF-κB activity in acute kidney injury. (A) *In vivo* bioluminescence whole-body imaging of *κ-Luc* mice following right uninephrectomy and sham surgery (control; upper panel) or 17.5 minutes left renal ischemia (lower panel). After the procedure, mice were imaged at time points stated below. (B) NF-κB-driven luciferase activity in sham operated mice (□, n=3) and in mice with ischemic kidney injury (■, n=4). *P<0.05, Student's t-test. (C) Immunostaining of contralateral kidney (non-injured; left panel) and of kidney 24 hours after ischemia (injured; right panel) with an antibody against phosphorylated (P) p65. G, glomeruli; Pt, proximal tubule, Dt, distal tubule; Cd, collecting duct. Black frames indicate sites of ×400 magnification. Yellow bars represent 1000 µm, black bars represent 50 µm. (D) Quantification of nuclear P-p65 staining in cortex (left panel) and medulla (right panel). RCC; red channel count (see Concise Methods). $n_{Contralateral}$=4, $n_{Injured}$=4, #P<0.05, Mann-Whitney U-test.

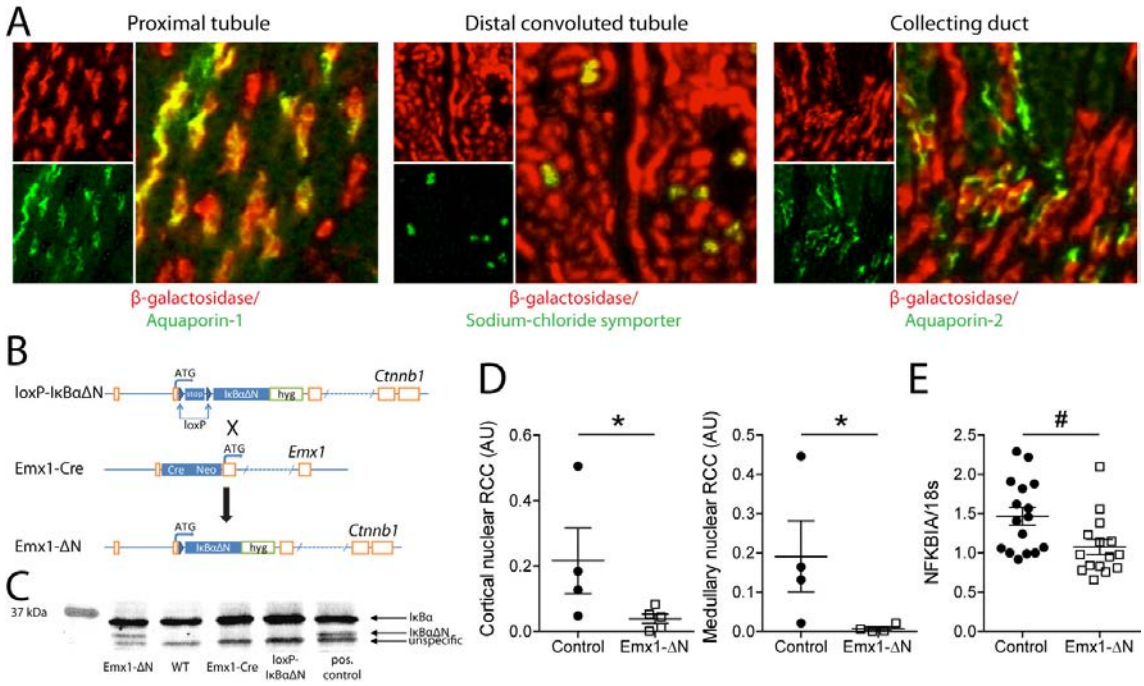

Figure 2. Generation and characterization of a mouse model with renal tubulus-specific expression of the human NF-κB super-repressor IκBαΔN. (A) Immunostaining on kidney sections from *Emx1Cre;R26R* mice using antibodies against β-galactosidase and aquaporin-1, sodium-chloride symporter or aquaporin-2 to verify renal tubular Cre activity. (B) The cDNA of the NF-κB super-repressor IκBαΔN was knocked into the *β-catenin* (Ctnnb1) locus preceded by a loxP-stop-loxP cassette (*loxP-IκBαΔN*). Mating of *loxP-IκBαΔN* with *Emx1-Cre* knock-in animals generated mice expressing IκBαΔN only in cells with an active Emx1 promoter (Emx1-ΔN). (C) Verification of renal IκBαΔN expression in *Emx1-ΔN* mice by Western blotting using an anti-IκBα antibody. Kidney tissue lysates isolated from *IκBαΔN*^{ubi} mice, which constitutively express IκBαΔN ubiquitously, served as positive control. (D) Quantification of nuclear P-p65 staining in cortex (left panel) and medulla (right panel) from control and *Emx1-ΔN* mice 24 hours after ischemia. RCC, red channel count (see Concise Methods). $n_{control}$=4, $n_{Emx1\text{-}\Delta N}$=5, *P<0.05, Mann-Whitney U-test. (E) Expression of NFKBIA mRNA in control and *Emx1-ΔN* kidneys after 24-hour ischemia. $n_{control}$=16, $n_{Emx1\text{-}\Delta N}$=15, #P<0.05, Student's t-test.

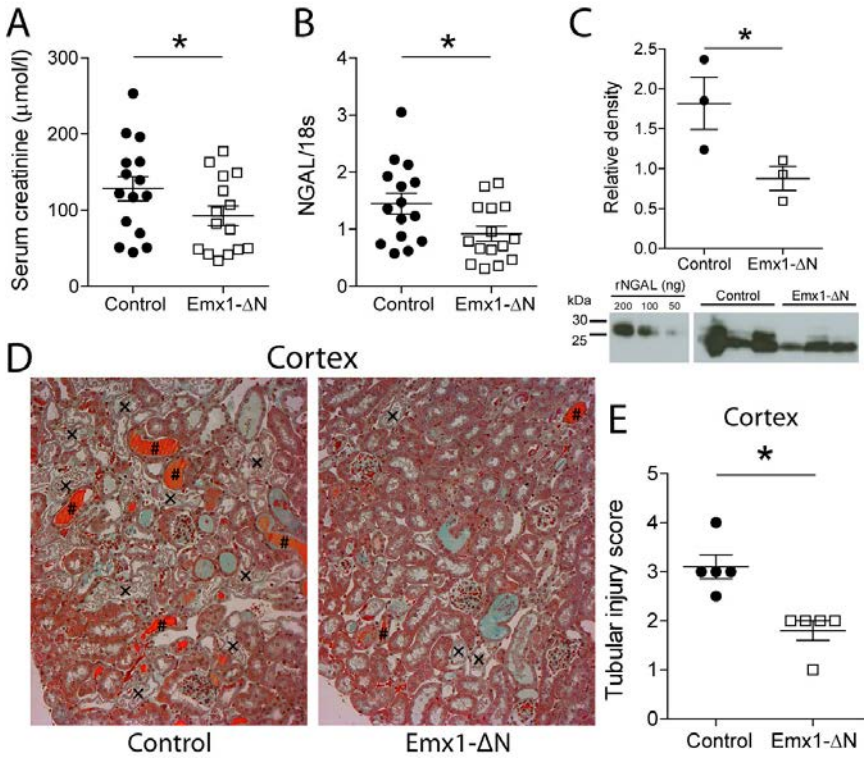

Figure 3. Suppression of NF-κB activity in renal tubules ameliorates acute kidney injury. (A) Serum creatinine levels and (B) mRNA levels of kidney injury marker neutrophil gelatinase-associated lipocalin (NGAL) in *Emx1-ΔN* mice and control littermates 24-hours after ischemia. $n_{Control}$=15, $n_{Emx1\text{-}\Delta N}$=15, *P<0.05, Student's t-test. (C) Urinary Western blot for analysis of NGAL expression using protein lysates from *Emx1-ΔN* mice and littermate controls. Recombinant mouse NGAL was used as a standard. $n_{Control}$=3, $n_{Emx1\text{-}\Delta N}$=3, *P<0.05, Student's t-test. (D) Representative images of Masson's trichrome stain on kidney sections of controls and *Emx1-ΔN* mice after 24 hours of ischemia (×400). Tubular necrosis (×) and eosinophilic cellular debris (#) are shown. (E) Semi-quantification of cortical tubular injury. $n_{Control}$=5, $n_{Emx1\text{-}\Delta N}$=5, *P<0.05, Student's t-test.

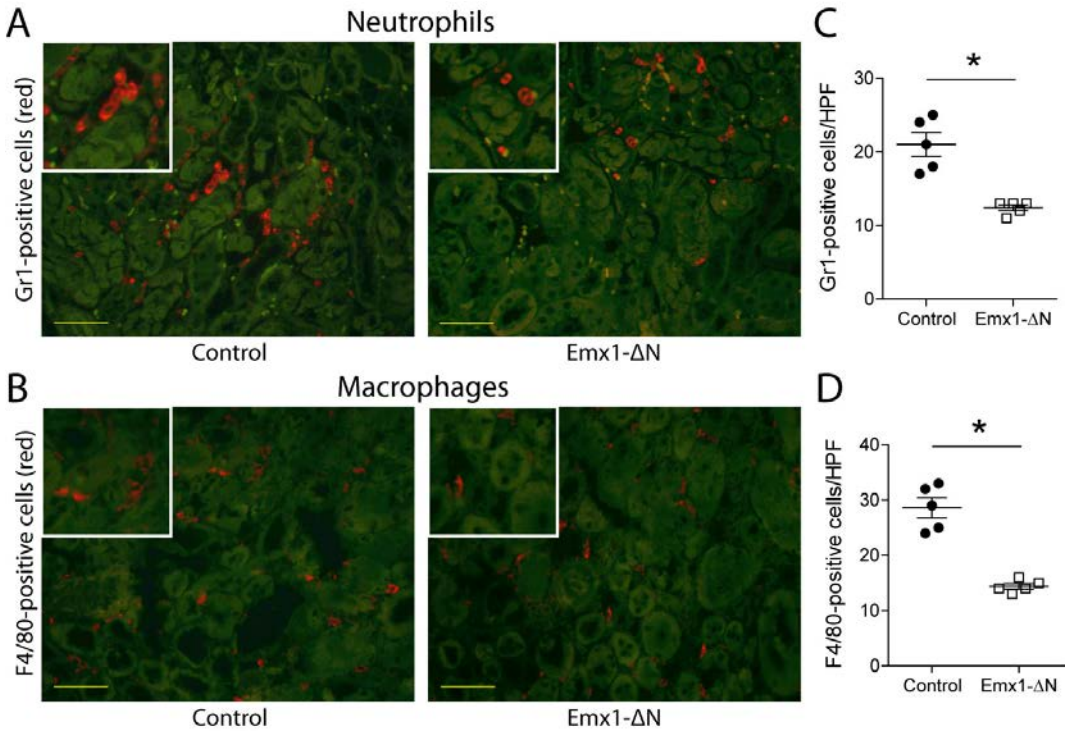

Figure 4. Inhibition of NF-κB activity in renal tubules is associated with reduced cellular infiltration after acute kidney injury. Immunofluorescence staining for neutrophil granulocyte marker Gr1 (red,(A)) and for dendritic cell/macrophage marker F4/80 (red,(B)) on representative kidney sections of control and *Emx1-ΔN* mice showing the outer medulla 24 hours after ischemia. Green staining is due to autofluorescence of tubules. Yellow bars represent 50 µm. Quantification of Gr1-positive (C) and F4/80-positive (D) cells. Each dot represents a single animal and is the mean of 20 randomly selected high-power fields (HPF). $n_{Control}$=5, $n_{Emx1\text{-}\Delta N}$=5, *P<0.05, Student's t-test.

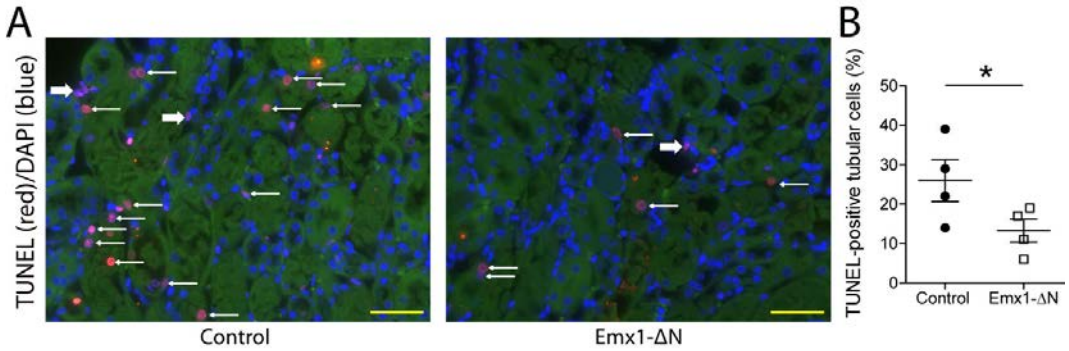

Figure 5. Inhibition of NF-κB activity in renal tubules leads to reduced apoptosis upon acute kidney injury. (A) Representative ×400 images of TUNEL labeling on control and *Emx1-ΔN* kidney sections 24-hours after renal ischemia. Thin white arrows indicate TUNEL-positive tubular cells. Thick white arrows indicate TUNEL-positive interstitial cells. Yellow bars represent 50 µm. (B) TUNEL labeling was quantified by direct counting of the number of positively stained tubular cells that was divided by the total number of cells per x630 field. Each dot represents a single animal and is the mean of 5 randomly selected outer medulla fields per animal. $n_{Control}$=4, $n_{Emx1\text{-}\Delta N}$=4, *P<0.05, Student's t-test.

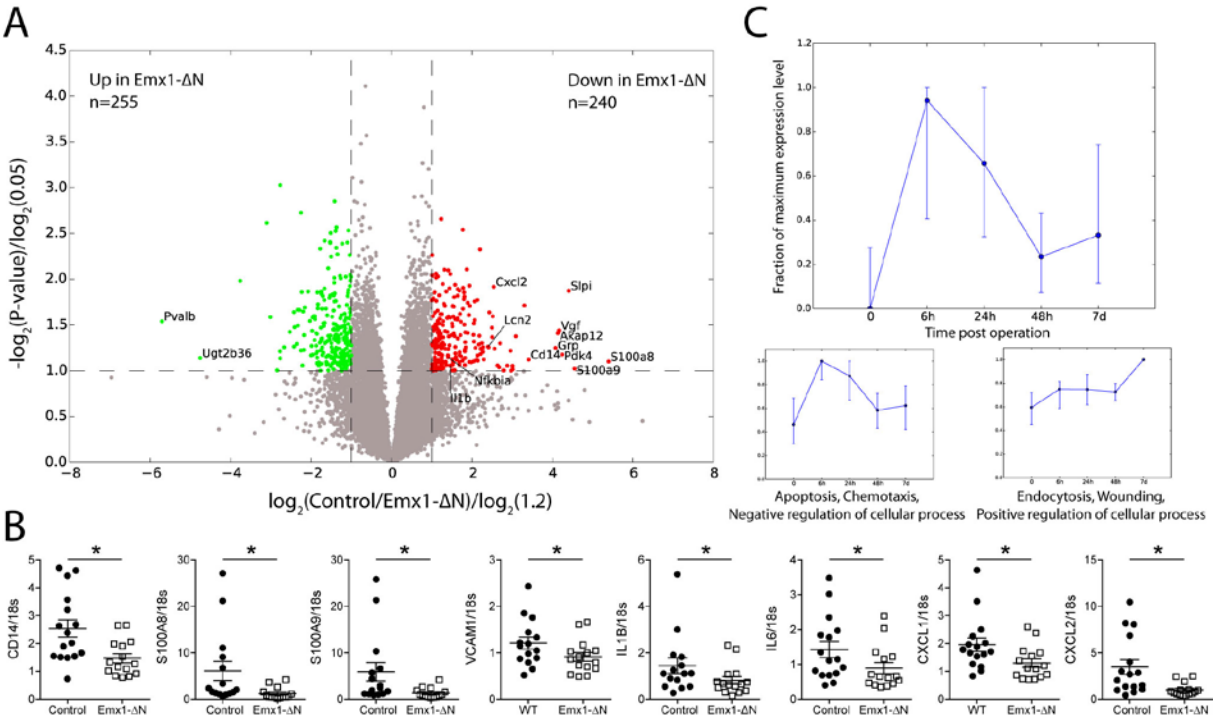

Figure 6. Microarray analysis comparing the gene expression profile of control versus *Emx1-ΔN* kidneys after ischemia. (A) Volcano plot for genes obtained from microarray analysis. Axes show logarithmic transformation of fold changes (x-axis) and P-values (y-axis). Genes differentially expressed (fold change>=1.2 and P-value<0.05) are in green if upregulated in *Emx1-ΔN* mice compared with controls, and in red if downregulated. (B) Verification by qRT-PCR of some of the NF-κB target genes downregulated in injured *Emx1-ΔN* kidneys. (C) Time-dependent expression pattern of all genes downregulated in injured kidneys of *Emx1-ΔN* mice compared with controls (red dots in (A)) at 0, 6h, 24h, 48h and 7d after ischemia. Displayed are time points 0, 6h, 24h, 48h and 7d. The upper panel shows median and quartiles for all differentially expressed genes downregulated in *Emx1-ΔN* when compared to control while the lower two panels are result of k-means clustering of these genes with respect to their time-wise expression pattern (see Methods for details). For each cluster, the dominant gene ontology (GO) term from gene ontology analysis and representative class members is depicted (for a full list of all members of each cluster and detailed result of GO analysis see Supplemental Table 2 and 3). All gene expression values have been maximum normalized for each gene.

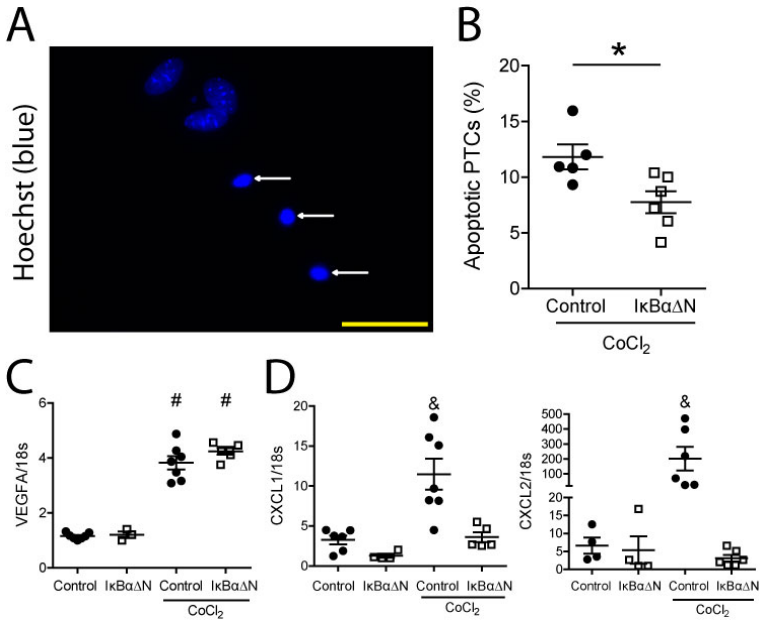

Figure 7. Primary proximal tubular cells (PTC) overexpressing IκBαΔN show less apoptosis and reduced chemotactic cytokine expression after $CoCl_2$ treatment. (A) Representative image of apoptotic PTC (white arrows) (x630). Yellow bar represents 50 µm. (B) Quantification of apoptotic PTC after a 24-hour treatment of 300 µM hypoxia-mimetic agent $CoCl_2$. Data of two independent experiments. $n_{Control}$=5, $n_{IκBαΔN}$ =6, *P<0.05, Student's t-test. mRNA expression of (C) HIF1α target gene VEGFA, and (D) chemokine CXCL1 and CXCL2. Each dot represents a pool of PTC isolated from 2-3 animals of the same genotype. Data of two independent experiments. $n_{Control}$=6, $n_{IκBαΔN}$ =4, $n_{Control+CoCl2}$=7 and $n_{IκBαΔN+CoCl2}$=6. , #P<0.05 versus WT and IκBαΔN, &P<0.05 versus WT, IκBαΔN and IκBαΔN+$CoCl_2$. One-way ANOVA, Newman-Keuls multiple comparison post-hoc test.